SURFACE AND INTERFACE ANALYSIS
Surf. Interface Anal. 2007; **39**: 161–165
Published online in Wiley InterScience
(www.interscience.wiley.com) DOI: 10.1002/sia.2482

Surface and Interface Analysis

The mobility of an alkali promoter as probed *in situ* during a catalytic reaction: Li in the CO oxidation on Pt

Y. Suchorski,[1]* J. Beben,[2] A. Frac,[2] V. K. Medvedev[3] and H. Weiss[1]

[1] Chemisches Institut, Otto-von-Guericke-Universität Magdeburg, Universitätsplatz 2, D-39106 Magdeburg, Germany
[2] Institute of Experimental Physics Wroclaw University, pl. Maxa Borna PL50-204, Wroclaw, Poland
[3] Department of Chemical Engineering, University of Washington, Box 351750, Seattle, WA 98195-1750, USA

Received 14 July 2004; Revised 22 December 2004; Accepted 4 April 2006

Fluctuations of the local ion rate of Li^+ ions emitted during *in situ* monitoring of the catalytic CO oxidation on the nanofacets of a Pt field emitter tip with a lithium field desorption-microscope (Li-FDM) are utilized to study the Li surface diffusion. The 'virtual probe-hole' approach, which is based on the digitization of the Li-FDM video images, is used. This allows to analyze simultaneously the local fluctuations of ions originating from arbitrarily user-defined probed surface regions of nanometer size. The anisotropy of the Li diffusion on the spatially inhomogeneous Pt surface is directly proved and a slowing effect of the coadsorbed CO on the Li diffusion is observed. Copyright © 2007 John Wiley & Sons, Ltd.

KEYWORDS: carbon monoxide; oxidation; alkali promoter; field-desorption microscope; lithium; diffusion

INTRODUCTION

Alkali metals are widely used as promoters in technologically important catalytic reactions and thus various aspects of the alkali-caused effects on the catalytically active surfaces are being intensively studied nowadays.[1,2] An important, but often overlooked, factor in a promoted catalytic reaction is the mobility of the promoter itself, since a potential spatial redistribution of the promoting species during the reaction can drastically influence the reaction performance. Recent studies have focused therefore on the macroscopic mobility of the alkali atoms during the ongoing surface reaction, such as the catalytic H_2 oxidation on Rh. The redistribution of potassium under reaction conditions was observed by different spatially resolving methods such as SPEM (scanning photoelectron microscopy), MIEEM (metastable impact electron emission microscopy), and LEEM (low energy electron microscopy).[3–5] In a simplified way, this kind of redistribution, caused by a gradient of the chemical potential across the surface and kinetically controlled by the varying dopant diffusivity, can be traced back to the spinodal decomposition, which is well known as a three-dimensional (3D) effect and explained in terms of an 'up-hill diffusion'.[6,7] Only a few examples of a '2D projection' of this effect, such as concentration patterns of electropositive adsorbates resulting from the up-hill diffusion in two-dimensional first-order phase transitions under reaction-free conditions, are described in the literature.[8,9] A simple mathematical model, based on the phenomenological consideration of a strong affinity between potassium and oxygen and accounting for the differences in the mobility of alkali atoms on the oxidized and reduced surface, fits the experimental observations during the progressing H_2 oxidation.[10]

Most of the experimental results obtained till now were collected on well-defined macroscopic single-crystal surfaces, and are thus difficult to compare with real catalytic systems like oxide-supported small metal particles with a highly heterogeneous surface (materials gap problem). The most characteristic property of such a metal particle is the presence of differently oriented facets, which are confined by stepped regions. The surface of a field emitter tip exhibits a similarly heterogeneous surface formed by differently oriented nanofacets and can thus serve as a model for a catalytic particle of comparable dimensions. However, in contrast to a catalyst particle, the tip surface can be prepared reproducibly and can be characterized with atomic resolution by field ion microscopy (FIM). Using this and other field-emission-based techniques, such as field electron microscopy (FEM), one can follow dynamic processes like surface diffusion with a lateral resolution $\leq$2 nm.[11–13] Moreover, surface reactions such as the catalytic CO or H_2 oxidation can be visualized *in situ* on well defined nano-sized facets,[14,15] even in the presence of alkali promoters.[16]

In principle, the microscopic mobility of coadsorbed species, like alkali, can be studied *in situ* by FEM/FIM during the ongoing catalytic reaction by the same methods as under reaction-free conditions, i.e. for example by density fluctuation measurements.[11,13] In this case, however, the conventional FEM approach is not so helpful since the fluctuations of the electron emission rate can also be caused by diffusion of CO or even oxygen as well as by the reaction itself.[17] In the present study, we have therefore used the fluctuations of the Li^+ ion rate, i.e. those of the field-desorbed ions of the promoter itself, in order to study its mobility under

*Correspondence to: Y. Suchorski, Chemisches Institut, Otto-von-Guericke-Universität Magdeburg, Universitätsplatz 2, D-39106 Magdeburg, Germany.
E-mail: yuri.suchorski@vst.uni-magdeburg.de

Copyright © 2007 John Wiley & Sons, Ltd.

WILEY InterScience® DISCOVER SOMETHING GREAT

Surface and Interface Analysis

reaction conditions. The depletion of the probed surface by desorption of Li is compensated by the continuous Li diffusion supply from the tip shank, similar to the one that takes place in the case of the CO^+ desorption in the FIM with carbon monoxide as imaging gas.[18]

Owing to the strong ionic component in their adsorption bonds, lithium adatoms can be desorbed from a metal surface by a relatively low external electric field of 0.5–1 V/Å even at cryogenic temperatures.[19] This allows to achieve measurable Li^+ field-desorption rates which can be utilized for the visualization of the adsorption sites on the surface, as already proposed by Müller in 1951.[20] The principal realizability was demonstrated a decade later,[21] but only the introduction of channel-plate-based image intensifiers finally allowed the development of a 'fully fledged' device, the lithium field-desorption microscope (Li-FDM) with a continuous imaging mode. The latter made possible the visualization of the dynamic surface processes using the Li^+ ions as the imaging species.[22] With this technique, surface reactions such as the CO oxidation on Pt or Rh surfaces can also be visualized *in situ*.[23,24]

In the present study, we report on the first attempt to monitor the surface diffusion of Li during the Li-modified catalytic CO oxidation on Pt with the Li-FDM. This became possible by adopting the 'virtual probe-hole' technique, which has been exploited before in our FEM study of Li diffusion under reaction-free conditions.[25] The idea behind it, namely, that the local image brightness fluctuations in the recorded Li-FDM video images can provide the surface diffusion parameters, is based on Onsager's hypothesis about the applicability of macroscopic diffusion laws to the microscopic density fluctuations,[26] and on the cognition that such brightness fluctuations reflect microscopic concentration deviations in an apparently homogeneous adsorbed layer and can thus be analyzed via the density fluctuation method, as first proposed.[25] The latter has already found use in FEM probe-hole measurements[11,13] as well as in STM studies.[27] Its application to the Li-FDM allows the utilization of the full potential of the 'parallel'-imaging principle of this microscope (as of any field-emission-based microscope), and renders the simultaneous analysis of processes on different surface regions of only a few nm^2 size on the Pt tip possible, in contrast to the 'real probe-hole' measurements, where the emission from just one or two regions (in a 'two probe-holes' experiment[28]) can be measured. More details of the 'virtual probe-hole approach' can be found elsewhere.[13]

EXPERIMENTAL

The Li-FDM apparatus, which is based on a standard FIM in a bakeable UHV system, is described in detail elsewhere,[22] and only the principle of operation is outlined here. In the Li-FDM mode, lithium adatoms are field desorbed from the apex of the tip as Li^+ ions that in turn create a (channel-plate intensified) projection of the adsorption sites on the fluorescent screen (see Fig. 1). Removed Li adatoms are replaced by diffusion of Li along the tip from the long-lasting Li deposit on its shank. Since the tip assembly allows

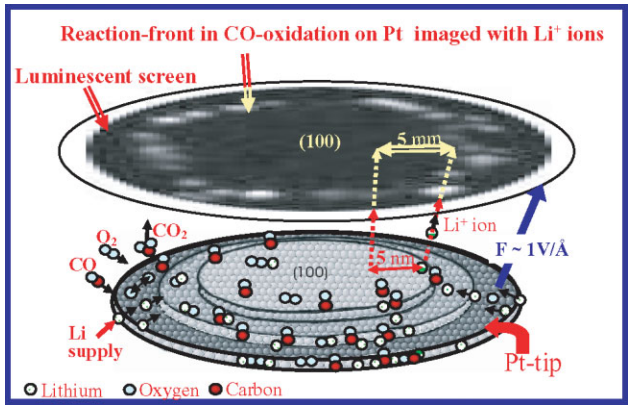

Figure 1. Imaging of the CO oxidation reaction in a lithium field desorption microscope (Li-FDM). Li adatoms, which are field desorbed from the apex of the tip as Li^+ ions, project an (channel-plate intensified) image of the adsorption sites onto the fluorescent screen. Removed Li adatoms are replaced by diffusion of Li along the tip from the long-lasting Li deposit on its shank. This figure is available in colour online at www.interscience.wiley.com/journal/sia.

controlled liquid nitrogen cooling as well as direct current heating and thus an operating temperature between 78 and 600 K (measured by a thermocouple immediately adjacent to the tip), the rate of the surface diffusion supply of Li to the imaged surface sites can be adjusted. The Li^+ desorption rate can be controlled by the externally applied field (usually 5 to 10 V/nm) and by the tip temperature. A submonolayer Li deposit (0.1–0.4 ml) is evaporated onto a Pt field emitter tip from a commercial Li source (SAES Getters). The resulting Li coverage can be estimated from the work function measured in the FEM mode, which can be switched on by simply reversing the tip voltage polarity.

The system was equipped with a gas supply system for an imaging gas (Ne, for the FIM imaging of the tip structure) and the gases used in the reaction (CO, O_2).

The specifics of the visualization of the CO oxidation reaction by Li-FDM are described explicitly in the literature.[23,24] The Li-FDM images were recorded during the ongoing reaction by means of a CCD camera with 40-ms time resolution and was digitized with eight-bit resolution. Certain rectangular probe regions (ROIs – 'regions of interest') were set, whose location and size were determined by overlapping the Li-FDM image with a low-temperature FIM image of the same tip. The size of the probed area was equal to or less than about 500 nm^2 in the experiments reported herein; mainly rectangular slit-like ROIs (e.g. 12 × 40 nm^2) were set. We note that the particular Pt-tip was blunted by the ongoing reaction at elevated temperatures as well as by the cleaning procedures to the radius of ~290 nm. Such a 'virtual slit probe-hole' can also be rotated within the digitizing procedure, thus allowing to study the anisotropy of diffusion as was shown before for a real slit-like probe-hole.[29,30] More details of the digitization procedure can be found elsewhere.[13,24]

RESULTS AND DISCUSSION

For the evaluation of the diffusion measurements, the autocorrelation function was used, similar to the early

Copyright © 2007 John Wiley & Sons, Ltd.

DOI: 10.1002/sia

experiments by Gomer using the conventional probe-hole technique.[29] With the corresponding calibration, the current fluctuations can be related to the fluctuations of the number of adatoms N in the probed area,[29] whose autocorrelation function is $A_N(t) = \langle \delta N(t+t')\delta N(t')\rangle'_t$, where $\delta N(t)$ is the fluctuation of N at time t and $\langle\rangle'_t$ denotes the average over t'. In the hydrodynamic regime, the autocorrelation function is related to the diffusion coefficient via

$$A_N(t) = (\langle N\rangle/A)\int_A\int_A (1/4\pi Dt)\exp(-|r-r'|^2/4Dt)d^2r d^2r' \quad (1)$$

where the integration over r and r' is carried out throughout the entire area A.[11,12] The experimentally obtained autocorrelation function is then compared to the theoretical curve derived from Smoluchowski's theory of density fluctuations, and the diffusion coefficient D is obtained from the comparison.[11–13] We have already applied this approach to the study of local FEM image brightness fluctuations exploiting the fact that the latter follow the adsorbate density fluctuations via the associated work function changes.[24] It is challenging to apply this approach also to field-desorbed ions instead of electrons. The investigation of field-ion rate fluctuations directly measured via the 'real probe-hole' technique has given evidence that such measurements permit the determination of the local diffusivities of the field-ionized adsorbed species, provided the field ionization occurs via the field-desorption mechanism (e.g. for CO molecules).[18] In the present work, we evaluate the autocorrelation functions of the local brightness of the image created by Li^+ ions field desorbed from the surface.

In Fig. 2, the reaction front in the CO oxidation reaction on a [100]-oriented Pt tip is imaged with Li^+ ions for the inactive (CO-covered; Fig. 2(a)) as well as for the active (oxygen-covered; Fig. 2(b)) state of the reaction. Below the Li-FDM images, the typical intensity fluctuation series are shown together with the corresponding fluctuation amplitude distributions for both cases. In the inactive state of the reaction, the fluctuations in the image originate mainly from the Li diffusion.[31] In contrast, in the active state, they are mainly caused by the reaction itself, are slower, and display larger amplitudes as well as non-Gaussian amplitude distributions peculiar to noise-induced transitions (see also Refs 31,32). In the following, we will concentrate on the inactive, CO-covered surface only. For more details of the reaction-induced fluctuations, we refer to the review.[33]

In Fig. 2(a), two different ROIs for the diffusion measurements are shown: in the ROI labeled 1, diffusion along the atomic steps confining the (111) facet is monitored, and in position 2, across the steps (please note that the diffusion is probed parallel to the shorter side of the respective ROIs). The corresponding experimental autocorrelation functions, which are shown in Fig. 3 together with the theoretical curves, demonstrate the differences in the diffusivity of Li on the CO-covered Pt(111) surface along and across the atomic steps. As expected, with $D^{\parallel} = 8 \times 10^{-13}$ cm^2/s, the diffusion along the steps is significantly faster than across them where values of $D^{-} = 2 \times 10^{-13}$ cm^2/s were obtained.

We note that the experimental error in the absolute values of D caused by known problems in the tip-radius estimation contributes with an uncertainty of $\sim 0.5 \times 10^{-13}$ cm^2/s to the D in all cases, but the ratio $D^{\parallel}/D^{-}$, important for the activation energy calculations, can be evaluated more reliably (with an accuracy of ~20%) with this method.

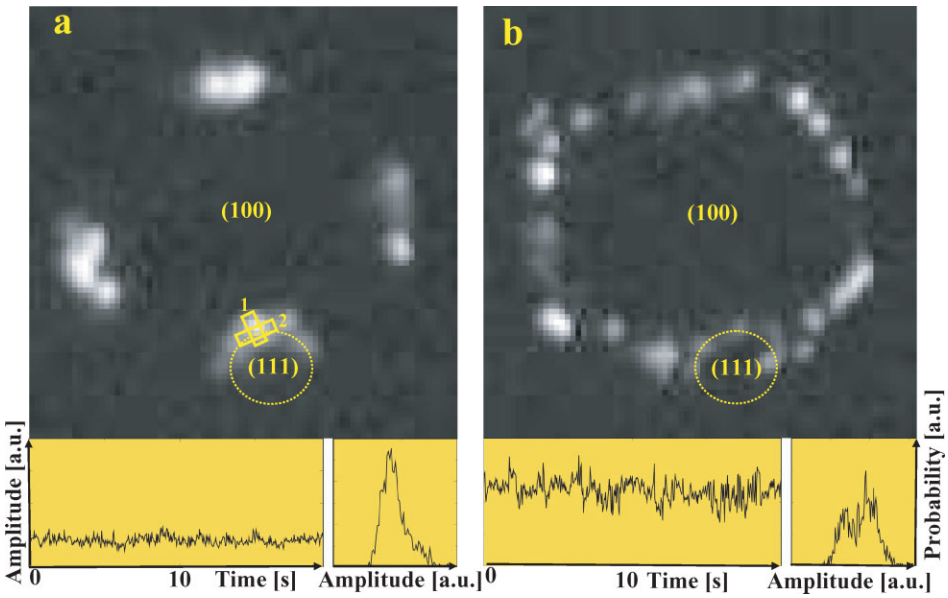

Figure 2. Reaction front and intensity fluctuations in the CO oxidation on a [100]-oriented Pt tip imaged with Li^+ ions in the Li-FDM mode. $T = 498$ K, $p_{CO} = 1.8 \times 10^{-5}$ mbar, $p_{O2} = 6.3 \times 10^{-5}$ mbar. (i) In the inactive (CO-covered) state, fluctuations of the image originate from Li diffusion. The ROI in the position 1 allows to monitor the diffusion along the atomic steps which confine the (111) facet, the ROI in position 2 across the steps, correspondingly. An example of a locally measured time series and a corresponding (Gaussian-like) amplitude distribution is shown below. (ii) In the active (oxygen-covered) state, fluctuations of the image are caused by the reaction itself. The corresponding local time series exhibits a bimodal (non-Gaussian) distribution. This figure is available in colour online at www.interscience.wiley.com/journal/sia.

Copyright © 2007 John Wiley & Sons, Ltd.

DOI: 10.1002/sia

Surface and Interface Analysis

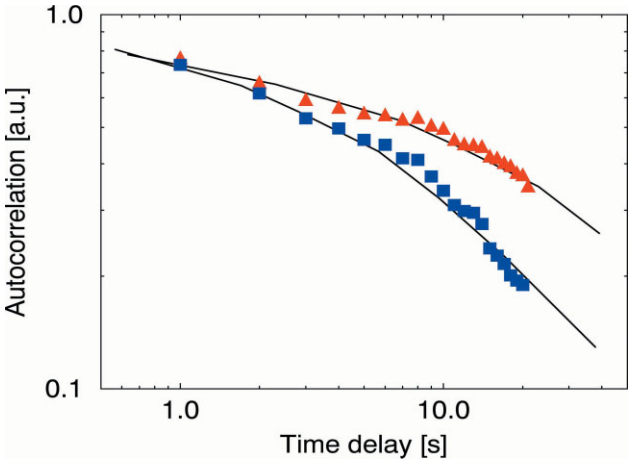

Figure 3. Autocorrelation functions which demonstrate the differences in the diffusivity of Li on the CO-covered Pt(111) surface along (■) and across (▲) the atomic steps. The diffusion coefficients ($D = 8 \times 10^{-13}$ and 2×10^{-13} cm^2/s, respectively) are derived from the theoretical autocorrelation functions fitting the experimental data. This figure is available in colour online at www.interscience.wiley.com/journal/sia.

In the discussion of the present results on the surface diffusion of Li on the CO-covered Pt(111) nanofacet, it has to be taken into account that here the potential barrier for the Li diffusion is mainly governed by the structure of the atomic steps present on the apex of a [100]-oriented Pt tip. For this reason, the obtained diffusivity values have to be compared with caution to data measured for macroscopic single crystals. In principle, additional effects can be caused by the applied electric field of about 5 V/nm in the Li-FDM mode, which may possibly slightly influence the diffusivity of Li on these surfaces.[34] However, a field effect, if present at all, is not a peculiarity of the present 'virtual probe-hole' measurements, but is a general feature of all field-emission based methods.

Unfortunately, apart from our earlier FEM study,[24] the surface diffusion of Li has so far not been studied on stepped single-crystal surfaces, neither clean, nor covered with coadsorbed CO. The comparison of the diffusion coefficients obtained here for the CO-covered surface shows that these are generally lower than those measured on clean Pt surfaces[35] (including the stepped surface of a Pt field emitter tip),[24] where they range between 10^{-12} and 10^{-9} $cm^2 \cdot s^{-1}$ at similar temperatures. This is understandable and is due to the presence of adsorbate–adsorbate (Li-CO) interactions as well as because of the modified energetics of the Li adsorption on the Pt surface under the given reaction conditions. The observed variations of the diffusivity across and along the atomic steps can be explained on the basis of different activation energies, as recently predicted from Monte–Carlo simulations of a lattice-gas model.[36]

CONCLUSIONS

It has been demonstrated that the correlation analysis of the brightness fluctuations in a Li-FDM image can be employed for the *in situ* determination of the surface diffusivity of an alkali coadsorbate (Li), which is used as a dopant in a surface reaction. The anisotropy of the Li diffusion on the spatially inhomogeneous Pt surface (stepped nanofacets of a field emitter tip) was directly proved and a slowing effect of the coadsorbed CO on the Li diffusion was observed. Although the range of measurable diffusion coefficients was restricted in the present experiments to values less than 10^{-9} cm^2/s due to the time resolution of the image-recording process (40 ms/frame), significantly faster diffusion processes can be investigated when high-speed cameras are employed.

Recently it was shown that catalyst nanoparticles exhibit a similar relative amplitude of adatom density fluctuations[37] and a similar geometry of the stepped terraces. We therefore expect the results of our study not only to be valid for the nanosized surfaces on the apex of a field emitter tip but also for 'real-world' systems which also exhibit Pt(111) orientations. The future use of the fluctuation analysis, as applied in the present article, seems also possible on the heterogeneous supported catalysts, provided experimental techniques are developed, which permit the *in situ* monitoring of such fluctuations in realistic systems.

Acknowledgements

Technical assistance by Michael Schulz in digitizing the video tapes is gratefully acknowledged. This work was partially supported by the Wroclaw University under Project No. 2016/W/IFD/02. J.B. would like to thank the University of Magdeburg for a travel grant.

REFERENCES

1. Kiskinova MP. In *Poisoning and Promotion in Catalysis Based on Surface Science Concepts and Experiments*, *Studies in Surface Science and Catalysis*, vol. 70, Kiskinova MP (ed.). Elsevier: Amsterdam, 1989.
2. Janssens TVW, Wandelt K, Niemantsverdriet JW. *Catal. Lett.* 1993; **19**: 263, and references therein.
3. Marbach H, Günter S, Luerssen B, Gregoratti L, Kiskinova M, Imbihl R. *Catal. Lett.* 2002; **83**: 161.
4. Lilienkamp G, Han Wei, Maus-Friedrichs W, Kempter V, Marbach H, Guenther S, Suchorski Y. *Surf. Sci.* 2003; **532–535**: 132.
5. Marbach H, Lilienkamp G, Wei H, Guenther S, Suchorski Y, Imbihl R. *Phys. Chem. Chem. Phys.* 2003; **5**: 2730.
6. Dehlinger U. *Z. Phys. Chem. Unterr.* 1937; **50**: 134.
7. Seith W. *Diffusion in Metallen*. Springer: Berlin, 1955; and references therein.
8. Naumovets AG. In *The Chemical Physics of Solid Surfaces*, vol. 7, King DA, Woodruff DP (eds). Elsevier: Amsterdam, 1994; 163.
9. Lyuksyutov I, Naumovets AG, Pokrovski V. *Two-Dimensional Crystals*. Academic Press: Boston, 1992.
10. Hinz M. *Numerical Simulation of the Pattern Formation in Heterogeneous Catalysis on the Rh(110) Surface*. Ph.D. Thesis, University of Hanover, Hanover, 2003.
11. Mazenko G, Banavar JR, Gomer R. *Surf. Sci.* 1981; **107**: 459.
12. Gomer R. *Rep. Prog. Phys.* 1990; **53**: 917.
13. Suchorski Y, Beben J. *Progr. Surf. Sci.* 2003; **74**: 3, and references therein.
14. Gorodetskii V, Drachsel W, Block JH. *Catal. Lett.* 1993; **19**: 223.
15. Gorodetskii V, Lauterbach J, Rotermund HH, Block JH, Ertl G. *Nature* 1994; **370**: 277.
16. Medvedev VK, Suchorski Yu. *Surf. Sci.* 1996; **364**: L540.
17. Suchorski Y, Beben J, Imbihl R, James EW, Liu D-J, Evans JW. *Phys. Rev.* 2001; **B63**: 165417.
18. Suchorski Y, Beben J, Medvedev VK, Block JH. *Appl. Surf. Sci.* 1996; **94/95**: 207.
19. Suchorski Yu, Medvedev VK, Block JH, Wang RLC, Kreuzer HJ. *Phys. Rev.* 1996; **B53**: 4109.

Copyright © 2007 John Wiley & Sons, Ltd.

DOI: 10.1002/sia

20. Müller EW. *Z. Phys.* 1951; **131**: 533.
21. Gavriliuk VM, Medvedev VK. *Sov. Phys. Tech. Phys.* 1966; **11**: 1282.
22. Medvedev VK, Suchorski Yu, Block JH. *Ultramicroscopy* 1994; **53**: 27.
23. Medvedev VK, Suchorski Yu, Block JH. *Appl. Surf. Sci.* 1994; **76/77**: 136.
24. Medvedev VK, Suchorski Yu, Block JH. *Appl. Surf. Sci.* 1995; **87/88**: 159.
25. Suchorski Y, Beben J, Imbihl R. *Ultramicroscopy* 1998; **73**: 67.
26. Onsager L. *Phys. Rev.* 1931; **38**: 2265.
27. Losano ML, Tringides MC. *Europhys. Lett.* 1995; **30**: 537.
28. Beben J, Kleint C, Meclewski R. *Surf. Sci.* 1989; **213**: 438.
29. Gomer R. *Surf. Sci.* 1973; **38**: 373.
30. Tringides M, Gomer R. *Surf. Sci.* 1985; **105**: 254.
31. Suchorski Y, Beben J, Imbihl R. *Surf. Sci.* 1998; **405**: L477.
32. Suchorski Y, Beben J, James EW, Evans JW, Imbihl R. *Phys. Rev. Lett.* 1999; **82**: 1907.
33. Suchorski Y, Beben J, Imbihl R. *Prog. Surf. Sci.* 1998; **59**: 343.
34. Suchorski Y. *Acta Phys. Pol.* 1992; **A81**: 295.
35. Naumovets AG, Zhang Z. *Surf. Sci.* 2002; **500**: 414, references therein.
36. Mašín M, Vattulainen I, Ala-Nissila T, Chvoj Z. *Surf. Sci.* 2004; **566–568**: 143.
37. Johanek V, Laurin M, Grant AW, Kasemo B, Henry CR, Libuda J. *Science* 2004; **304**: 1639.

Copyright © 2007 John Wiley & Sons, Ltd.